GEOPHYSICAL RESEARCH LETTERS, VOL. 36, L21702, doi:10.1029/2009GL040057, 2009



# Controls on Northern Hemisphere snow albedo feedback quantified using satellite Earth observations

Richard Fernandes,[1] Hongxu Zhao,[1] Xuanji Wang,[2] Jeff Key,[3] Xin Qu,[4] and Alex Hall[4]

Received 13 July 2009; revised 1 October 2009; accepted 12 October 2009; published 5 November 2009.

[1] Observation based estimates of controls on snow albedo feedback (SAF) are needed to constrain the snow and albedo parameterizations in general circulation model (GCM) projections of air temperature over the Northern Hemisphere (NH) landmass. The total April-May NH SAF, corresponding to the sum of the effect of temperature on surface albedo over snow covered surfaces ('metamorphism') and over surfaces transitioning from snow covered to snow free conditions ('snow cover'), is derived with daily NH snow cover and surface albedo products using Advanced Very High Resolution Radiometer Polar Pathfinder satellite data and surface air temperature from ERA40 reanalysis data between 1982–1999. Without using snow cover information, the estimated total SAF, for land surfaces north of 30°N, of $-0.93 \pm 0.06\%K^{-1}$ was not significantly different (95% confidence) from estimates based on International Satellite Cloud Climatology Project surface albedo data. The SAF, constrained to only snow covered areas, grew to $-1.06 \pm 0.08\%K^{-1}$ with similar magnitudes for the 'snow cover' and 'metamorphosis' components. The SAF pattern was significantly correlated with the 'snow cover' component pattern over both North America and Eurasia but only over Eurasia for the 'metamorphosis' component. However, in contrast to GCM model based diagnoses of SAF, the control on the 'snow cover' component related to the albedo contrast of snow covered and snow free surfaces was not strongly correlated to the total SAF. **Citation:** Fernandes, R., H. Zhao, X. Wang, J. Key, X. Qu, and A. Hall (2009), Controls on Northern Hemisphere snow albedo feedback quantified using satellite Earth observations, *Geophys. Res. Lett.*, *36*, L21702, doi:10.1029/2009GL040057.

## 1. Introduction

[2] Changes in planetary albedo due to changes in snow and ice cover induced by increasing surface air temperature ($T$ [°K]) can result in increased absorbed solar radiation [*Wexler*, 1953]. Early planetary energy budget models [*Budyko*, 1969; *Sellers*, 1969] predicted that the subsequent increase in radiation would complete a positive planetary albedo feedback (PAF) loop [*Lian and Cess*, 1977] by leading to an increase in $T$. Equilibrium $2 \times CO_2$ [*Hall*, 2004] and transient Intergovernmental Panel on Climate Change (IPCC) general circulation model (GCM) experiments have demonstrated that the April–May average (springtime) PAF explains close to half the increase in northern hemisphere $T$ response to anthropogenic forcings [*Hall and Qu*, 2006; *Winton*, 2006] and approximately one third of the increase over the Arctic [*Graversen and Wang*, 2009]. Observations [*Qu and Hall*, 2006, hereafter QH2006] and GCM experiments [*Winton*, 2006; QH2006] confirmed the hypothesis of *Lian and Cess* [1977] that temporal variability in surface albedo related to temperature changes over seasonally snow and ice covered land areas - the snow albedo feedback (SAF) - explains the majority of the variability of the global mean annual PAF. The strength of the SAF is given by [*Lian and Cess*, 1977; QH2006]:

$$\left(\frac{\partial \overline{Q}}{\partial \overline{T}}\right)_{SAF} = -\overline{I}\frac{\partial \overline{\alpha}_p}{\partial \overline{\alpha}_s}\frac{d\overline{\alpha}_s}{d\overline{T}} \quad (1)$$

where $Q$ [$Wm^{-2}$] is net shortwave radiation and the overbar corresponds to insolation ($I$ [$Wm^{-2}$]) weighted averages for planetary albedo $\alpha_p$ [%] and surface albedo $\alpha_s$[%] and spatial averages for $Q$, $T$ and $I$.

[3] The regionally averaged SAF sensitivity is $d\overline{\alpha}_s/d\overline{T}$ [$\%K^{-1}$] [QH2006]. QH2006 found that differences in the springtime SAF sensitivity (hereafter simply SAF) over the land regions north of 30°N (hereafter NH30), rather than controls of the atmosphere on the relationship between average surface and planetary albedo, explained the majority of the differences in SAF among IPCC Fourth Assessment Report (AR4) model projections for a given scenario. As such, observational constraints on SAF sensitivity within these transient models runs could potentially reduce the uncertainty in projected $T$ changes over the NH.

[4] *Hall and Qu* [2006] showed that April-May SAF computed from AR4 model 20th to 21st century equilibrium climate change runs is linearly related to the seasonal SAF from 20th century runs. *Hall et al.* [2008, hereafter H2008] used observations of surface albedo (International Cloud Satellite Climatology Project, ISCCP [*Zhang et al.*, 2004]) and reanalysed estimates of $T$ (ERA40 [*Simmons and Gibson*, 2000]) to quantify NH SAF between 1984–2000 using an updated conversion of narrowband to shortwave clear-sky albedo with the ISCCP dataset.

[5] *Qu and Hall* [2007, hereafter QH2007], related SAF to the local snow cover sensitivity, defined as the change in snow cover versus change in $T$ using two feedback control factors: 'metamorphosis' and 'snow cover'. They quantified the NH average equivalents for these local components using March-May IPCC GCM outputs over the 20th and 21st century. They found that the 'snow cover' component of the SAF and specifically the snow cover control factor related

[1]Canada Centre for Remote Sensing, Earth Sciences Sector, Natural Resources Canada, Ottawa, Ontario, Canada.
[2]Cooperative Institute for Meteorological Satellite Studies, University of Wisconsin-Madison, Madison, Wisconsin, USA.
[3]NESDIS, NOAA, Madison, Wisconsin, USA.
[4]Department of Atmospheric and Oceanic Sciences, University of California, Los Angeles, California, USA.


0094-8276/09/2009GL040057$05.00

to albedo contrast of snow covered and snow free land explained most of the inter-model spread in SAF.

[6] The work of QH2007 and H2008 raises some important questions if modelers are to use observed controls on SAF to improve GCM projections. Firstly, will SAF differ substantially if calculated using recent all-sky albedo estimates rather than the ISCCP based estimates of H2008? Secondly, does the fact that the snow cover component explains inter-model spread in SAF imply it also explains observed spatial patterns in the SAF? Thirdly, are spatial patterns for observed multi-year mean springtime SAF components consistent from year to year and what is their variability due to internal climate variability?

## 2. Method

[7] The SAF sensitivity ($\overline{\kappa}_4^{-1}$ [%K$^{-1}$]) over a region $R$ is related to the local SAF sensitivity, $d\alpha_s(r)/dT(r)$ (denoted as $\kappa_4^{-1}$ [%K$^{-1}$]) as

$$\overline{\kappa}_4^{-1} = \frac{1}{\overline{A}} \int_R \kappa_4^{-1}(r) \frac{dT(r)}{d\overline{T}} P(r) dA(r) \tag{2}$$

where $P(r)$ [unitless] is the local planetary insolation relative to the average over $R$ and $dA(r)$ is the local contribution to total surface area $\overline{A}$ [m$^2$]. Assuming, as QH2007 do, that snow metamorphosis and snow cover $S_c$ [%] changes are the main drivers of $\kappa_4^{-1}$ gives:

$$\kappa_4^{-1} = \kappa_3 + \kappa_2 \kappa_1 \tag{3}$$

where,

$$\kappa_1 = \frac{dS_c(r)}{dT(r)} \tag{4}$$

[%K$^{-1}$] is the snow cover sensitivity to temperature,

$$\kappa_2 = \frac{\partial \alpha_s(r)}{\partial S_c(r)} \approx \frac{\alpha^f_{snow} + \alpha^p_{snow}}{2} - \alpha_{land} \tag{5}$$

[unitless] is the snow cover feedback factor,

$$\kappa_3 = \frac{\partial \alpha_s(r)}{\partial T(r)} \approx \frac{S^f_c + S^p_c}{2} \frac{\alpha^f_{snow} - \alpha^p_{snow}}{\Delta T} \tag{6}$$

[%K$^{-1}$] is the metamorphosis component, $\alpha_{snow}$ [%] and $\alpha_{land}$ [%] are the surface albedo of snow covered and snow free surfaces respectively and '$f$' and '$p$' correspond to future and present climates. QH2007 estimated local SAF components by solving equations (3) through (6) for $\Delta\alpha_s$ and then applied equations (1) and (2) to quantify the contribution of each component to the NH30 averages. Our approach relies on seasonal observations with the analog for present and future conditions corresponding to April and May respectively.

[8] Coincident monthly averaged $T$, $\alpha_s$, and $S_c$ were derived for ERA40 2.5° grid cells between 1982 and 1999 from ERA40, Advanced Very High Resolution Radiometer (AVHRR) Polar Pathfinder-x (APP-x) all-sky albedo [*Wang and Key*, 2005] and Canada Centre for Remote Sensing NH APP Snow Cover [*Zhao and Fernandes*, 2009] products respectively. The latter two products were derived from AVHRR Polar Pathfinder (APP) data generated from the original 1 km resolution AVHRR imagery by sub-sampling every third line and retaining the average of the first four 1 km pixels in each non-overlapping five pixel segment along the line. Each averaged measurement at the nominal location of the corresponding 5 pixel segment was reprojected into the NH APP domain (NHAPP), defined as a 5 km resolution Equal Area Scaleable Earth Grid [*Maslanik et al.*, 1997; *Fowler et al.*, 2000] bounded at 29.74956°N latitude at corners and 48.40237°N latitude at edge centres. The APP snow cover product is derived for each APP pixel while the APP-x albedo was mapped at a fifth row and column sub sampling of the APP grid giving a 25 km × 25 km product. For consistency the APP snow cover product was also sub-sampled to the same grid as the APP-x albedo and a 2.5° × 2.5° moving average was then applied to both products.

[9] For each year, $\kappa_4^{-1}$ and $\kappa_1$ were estimated using changes in monthly average $T$, $\alpha_s$ and $S_c$ over each 2.5° grid cell. The average $\alpha_s$ for the first 30 consecutive snow free dates after March 31st was used to estimate $\alpha_{land}$ for each year. The coincident annual $\alpha_{snow}$ was estimated assuming a linear mixture model for grid cells with non-zero $S_c$:

$$\alpha_{snow} = [\alpha_s - (1 - S_c)\alpha_{land}]/S_c \tag{7}$$

Equation (5) was applied to estimate $\kappa_2$ and then $\kappa_3$ was quantified with equation (3). The NHAPP averages for $\kappa_3$ and $\kappa_1\kappa_2$ was estimated from equation (2).

[10] The interannual local mean and standard deviation ($\sigma$) of SAF components, weighted by $P(r)$ for $\kappa_1$ and $\kappa_2$ and $P(r)dT(r)/d\overline{T}$ for $\kappa_4^{-1}$, $\kappa_3$ and $\kappa_1\kappa_2$ were derived. Random observational errors will likely cancel for the NH average so $\sigma$ serves to quantify the impact of internal climate variability on each component (reported as the 95% confidence interval of the 18-year average). Spatial correlation coefficients ($\rho$) between unweighted interannual means of local SAF components were computed over both North America (NA) and Eurasia (EU) to isolate interrelationships of land surface dynamics. Henceforth we refer to weighted components except when discussing spatial correlations.

## 3. Results

### 3.1. Comparison of Observed and Modelled SAF Sensitivity

[11] The NHAPP $\overline{\kappa}_4^{-1}$, using satellite based albedo data and reanalysed temperature estimates, was $-1.11 \pm 0.07$%K$^{-1}$. Adjustment of this estimate for the NH30 domain, using zonal average $\kappa_4^{-1}$ to fill in missing grid cells, gives NH30 $\kappa_4^{-1}$ of $-0.93 \pm 0.06$%K$^{-1}$. The NH30 $\overline{\kappa}_4^{-1}$ lies below the ISSCP-FD estimate of $-1.13 \pm 0.13$%K$^{-1}$ and is not significantly different from the ISCCP-MODIS corrected estimate of $-0.91 \pm 0.11$%K$^{-1}$ given in H2008. All three estimates share the same ERA40 $T$ so remaining differences are likely due to the difference between ISCCP and APP-x $\alpha_s$ inputs or the approach used to estimate the NH average. Differences in albedo estimates may arise when approximating shortwave albedo from bandlimited spectral albedo estimates as documented in H2008 or due to differences in approaches used to estimate all-sky albedo based primarily

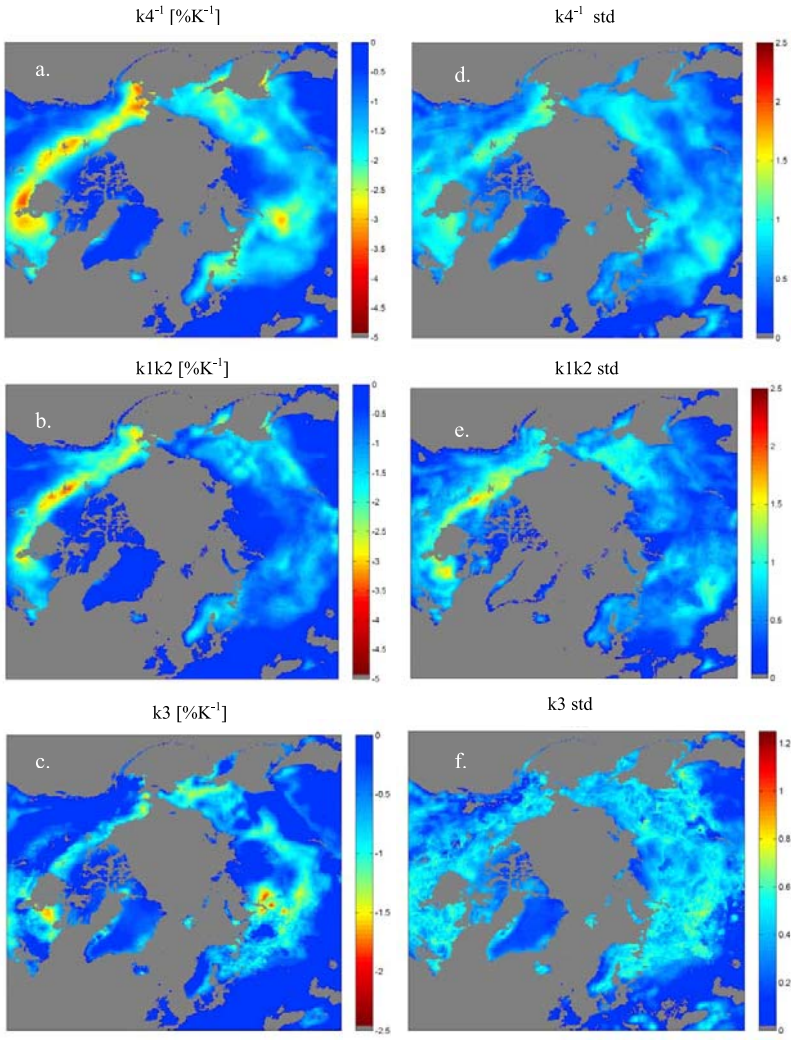


**Figure 1.** Spatial patterns of 18 year average April–May (a) total SAF sensitivity, (b) snow cover component and (c) metamorphosis component and (d–f) associated interannual standard deviation between 1982–1999.

on clear sky characterization of surface bi-directional reflectance distributions. It is noteworthy that our NH30 $\overline{\kappa_4}^{-1}$ shows reasonable agreement with early annual NH estimates by *Sellers* [1969] ($\sim -0.9\%K^{-1}$) and *Lian and Cess* [1977] ($\sim -1.0\%K^{-1}$) that were based on clear sky $\alpha_p$ from satellite observations and in-situ $T$ including regions covered by ice packs.

### 3.2. Separation of Snow Cover and Snow Metamorphosis Component

[12] The spatial patterns of local SAF components are shown in Figure 1. The total SAF sensitivity, $\kappa_4^{-1}$, lies between 0 and $-1\%K^{-1}$ except for a zonal belt just north of the tree line and over the western coastal mountains of NA ($-1$ to $-3\%K^{-1}$) containing isolated northern coastal regions where it reaches up to $-5\%K^{-1}$ (Figure 1a). The region of elevated $\kappa_4^{-1}$ is closely related to the $\kappa_2\kappa_1$ component in most of NA (Figure 1b) but there are regions (south of Hudson Bay, Canada, and northeastern and central Siberia) where the metamorphosis component drives the pattern if not the magnitude of $\kappa_4^{-1}$. Metamorphosis also plays a role in determining $\kappa_4^{-1}$ at the northern edge of this belt.

[13] The 18 year averages over the NHAPP for $\overline{\kappa_3}$ and $\overline{\kappa_2\kappa_1}$ were $-0.58 \pm 0.04\%K^{-1}$ and $-0.66 \pm 0.07\%K^{-1}$ respectively. Corresponding 18-year NH30 averages of $\overline{\kappa_3}$ and $\overline{\kappa_2\kappa_1}$ were $-0.52 \pm 0.04\%K^{-1}$ and $-0.54 \pm 0.07\%K^{-1}$ respectively. The magnitude of the sum of these components, $-1.06 \pm 0.08\%K^{-1}$, exceeds the NH30 $\overline{\kappa_4}^{-1}$ estimated directly from albedo and temperature since the latter includes regions that are snow free for both present and future months. As indicated in Table 1, over NA, the $\rho$ between $\kappa_2\kappa_1$ and $\kappa_4^{-1}$

**Table 1.** Spatial Autocorrelation Coefficients Between Interannual Average 2.5° Resolution Local SAF Components for North American and Eurasian NH Land Mass Regions[a]

| | $\kappa_4^{-1}$ | $\kappa_3$ | $\kappa_1\ \kappa_2$ | $\kappa_1$ | $\kappa_2$ |
|---|---|---|---|---|---|
| $\kappa_4^{-1}$ | | *0.72* | *0.65* | *0.44* | *−0.06* |
| $\kappa_3$ | **0.21** | | *−0.06* | *−0.04* | *0.13* |
| $\kappa_1\kappa_2$ | **0.80** | **−0.06** | | *0.68* | *−0.22* |
| $\kappa_1$ | **0.49** | **−0.57** | **0.80** | | *0.35* |
| $\kappa_2$ | **−0.20** | **−0.19** | **−0.07** | **0.35** | |

[a]Bold, North American; italics, Eurasian.

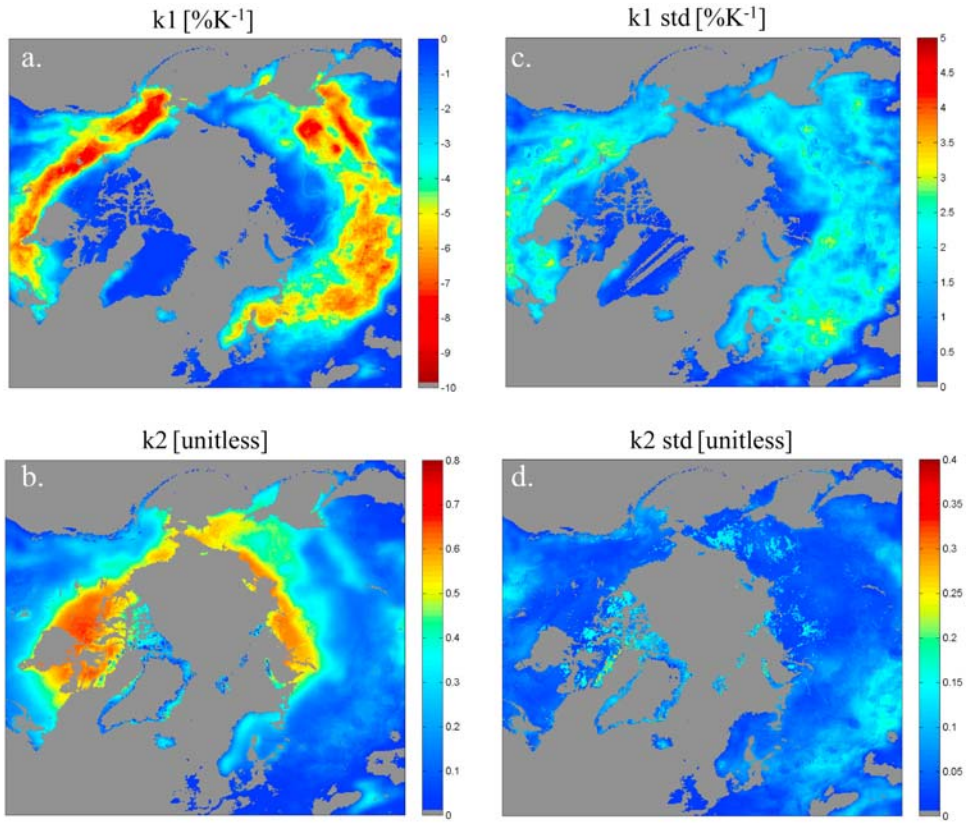


**Figure 2.** Spatial patterns of 18 year average April–May (a) snow cover sensitivity to temperature and (b) albedo sensitivity to snow cover and (c and d) associated interannual standard deviation between 1982–1999.

(0.80) was significantly larger than that between $\kappa_3$ and $\kappa_4^{-1}$ (0.21). This suggests that $\kappa_2\kappa_1$ explains the majority of both the average magnitude and spatial variability in $\kappa_4^{-1}$ over NA. In contrast, for EU, the $\rho$ of $\kappa_4^{-1}$ with $\kappa_3$ (0.72) is even larger than that with $\kappa_2\kappa_1$ (0.65) suggesting that metamorphosis and snow cover components contribute almost equally to $\kappa_4^{-1}$ here. Figure 1 indicates that $\kappa_3$ has similar magnitude as $\kappa_2\kappa_1$ at the northern edge of the melt zone and exceeds $\kappa_2\kappa_1$ in the Ungava peninsula in northern Quebec, Canada and in the Yamalo-Nenetskey Autonomous District of north eastern Russia. These regions are populated by small lakes where the satellite based snow cover estimates tend to bias towards later melt dates in the presence of sub-pixel (1 km × 3 km APP pixels) water cover [*Zhao and Fernandes*, 2009]. This may have resulted in reducing the snow cover component and, given our approach to estimate $\kappa_3$ as the residual of the SAF sensitivity and the snow cover component, would inflate $\kappa_3$. However, we would expect this behaviour in other areas of northern Canada where sub-pixel water fraction is equally large [*Fernandes et al.*, 2001]. It is also possible that the large metamorphosis detected in these regions corresponds to changes in albedo as snowpack depths drop and topographic shadowing increases. The patterns of large $\kappa_3$ magnitudes in Ungava and Siberia correlate qualitatively with patterns of surface radiative forcings caused by black carbon and mineral dust in snow presented by *Flanner et al.* [2009] suggesting that impurities in snowpack may also explain elevated metamorphosis factors.

[14] A spatial decomposition of $\kappa_2\kappa_1$ into $\kappa_1$ and $\kappa_2$ is shown in Figure 2. The relative contribution of both components to $\kappa_2\kappa_1$ cannot be compared in terms of NH averages since they act multiplicatively. However, their spatial cross-correlation to $\kappa_2\kappa_1$ (Table 1) clearly indicates that snow cover sensitivity $\kappa_1$ ($\rho$ = 0.68 to 0.80) rather than the snow albedo component, $\kappa_2$ ($\rho$ = −0.07 to −0.22), drives spatial patterns in $\kappa_2\kappa_1$. The smooth poleward increase in $\kappa_2$ (Figure 2b), suggests that it is actually the position of the maximum $\kappa_1$ values, the region with the highest temperature sensitivity (Figure 2a), that determines the spatial pattern of $\kappa_2\kappa_1$. The relatively weak observed spatial correlation between $\kappa_2\kappa_1$ and $\kappa_2$ contrasts with the finding by QH2007 that the spread in $\overline{\kappa}_2$ explained much of the spread in $\overline{\kappa}_4^{-1}$ within IPCC models. However, one must distinguish between causes of inter-model spread versus causes of actual spatial variability in SAF components. The former may simply reflect the fact that modelers do not have sufficient constraint on $\overline{\kappa}_2$ or that they are compensating for biases in other components. In reality $\kappa_1$ corresponds with Temperature Sensitive Regions (TSRs) [*Groisman et al.*, 1994] that have been related to NH SAF [*Déry and Brown*, 2007]. *Groisman et al.* [1994] placed the April–May TSRs to the north of our observational estimates. The observational estimates presented here are possibly more accurate that the estimates based on operational visual interpretation of satellite imagery reported by *Groisman et al.* [1994]. The observations also agree qualitatively with standardized climatological estimates of changes in $S_c$ between April and May [*Robinson and Frei*, 2000] and with TSRs [*Déry and Brown*, 2007; *Pielke et al.*, 2004] based on these data.

[15] The temporal coefficient of variation (c.v.) was 14% for $\overline{\kappa_4}^{-1}$, 16% for $\overline{\kappa_3}$, 21% for $\overline{\kappa_2\kappa_1}$, 4.6% for $\overline{\kappa_2}$ and 18% for $\overline{\kappa_1}$ over the NHAPP domain. The spatial correlation coefficient of mean and standard deviation patterns ranged from $-0.63$ to $-0.66$ indicating that all of the c.v.'s were relatively consistent spatially. However, $\kappa_2\kappa_1$ shows large (>2%K$^{-1}$) interannual variability in north western Russia, the Hudson Bay coastline and Labrador, Canada. These regions cannot be explained by the variability of either $\kappa_1$ or $\kappa_2$ separately (compare Figure 1d and Figures 2b and 2d) so it is due to a non-trivial interaction of these parameters. The stability of $\overline{\kappa_2}$ is evident in that it relates to land surface condition that we expect will change at longer time scales than our observation period. The moderate level of variability in $\overline{\kappa_4}^{-1}$ may be due to a negative correlation between variability in $\overline{\kappa_3}$ and $\overline{\kappa_2\kappa_1}$ (Table 1) that we hypothesize may also apply to interannual variability. Essentially, if snowpack albedo drops quicker in a given location or year so as to increase the metamorphosis component, the relative albedo change between snow free and snow covered ground will be lower so the snow cover component will tend to decrease.

## 4. Conclusions

[16] Following the suggestion of QH2007, spatial estimates of 18-year mean and standard deviations of April–May Northern Hemisphere SAF sensitivity and components were derived for the period 1982–1999 through the use of consistent snow cover and surface albedo datasets derived from APP data. The following conclusions are drawn from these observations:

[17] 1. The average NH April–May SAF ($\overline{\kappa_4}^{-1}$) between 1982 and 1999 based on the APP-x albedo and ERA40 temperature was $-1.11 \pm 0.07\%K^{-1}$ for the APP domain and $-0.93 \pm 0.06\%K^{-1}$ for the NH domain used by QH2007. The ISCCP-MODIS corrected based estimate for SAF [*Hall et al.*, 2008] was not significantly different with the APP estimates after accounting for biases in albedo definitions. The NH SAF estimated as the sum of snow cover ($\kappa_2\kappa_1$) and metamorphosis ($\kappa_3$) components is $-1.06 \pm 0.08\%K^{-1}$. This latter estimate, although not significantly different from the former estimates that do not use snow cover data, may be a more accurate characterisation of SAF since it excludes periods and regions where snow is absent. It is noteworthy that the early estimate of *Lian and Cess* [1977] based on somewhat different time periods, spatial domains and observational data was also not significantly different – in other words the scientific community had a good estimate available to it 30 years ago.

[18] 2. The NH average SAF sensitivity is equally explained by both snow cover ($\kappa_2\kappa_1$) and metamorphosis ($\kappa_3$) components. The North American spatial pattern of SAF is chiefly explained by the snow cover component but there is evidence that both snow cover and metamorphosis components contribute to the pattern of SAF over Eurasia. Anthropogenic deposition of impurities on central Eurasia snow covered surfaces may explain the distinction between the two continents. While snow melt sensitivity ($\kappa_1$) was correlated to spatial patterns in the snow cover component the snow albedo feedback ($\kappa_2$) was not. This may be due to the fact that, during April and May, the snow cover component is large north of the tree line where the spatial variability in the albedo contrast between snow covered and snow free conditions is relatively small.

[19] 3. The snow cover feedback and the total SAF showed moderate to low levels of interannual variability. These components might decouple with internal climate variability to some extent while the other SAF components exhibit larger sensitivity to internal climate variability. Nevertheless, even those SAF components that include substantial internal variability can be used to constrain models, albeit with reduced precision. More work is required to characterize the dependency of these components on internal climate variability in order to quantify the potential improvements in transient projections of models that are adjusted to agree with these observations.

[20] The IPCC has recognized the role of observations in constraining uncertainty in GCM projections [*Intergovernmental Panel on Climate Change*, 2007]. This study has derived observations of both hemispheric averages and spatial patterns of the components related to surface albedo feedback over northern land surfaces. The relatively low sensitivity of this feedback loop to internal climate variability facilitates the estimate of stable spatial averages from relatively short (18 years in our study) observational periods. These quantities can now be applied to assess GCMs and to provide guidance as to the role of physical mechanisms within the surface albedo feedback in a spatially explicit manner.

[21] **Acknowledgments.** The authors thank Ross Brown, Chris Fletcher and Paul Kushner for their comments and the Canadian International Polar Year Project 'Trends and Variability in the Canadian Cryosphere' and Natural Resources Canada Programme on Enhancing Canada's Resilience to Climate Change for financial support.

## References

Budyko, M. I. (1969), The effect of solar radiation variations on the climate of the Earth, *Tellus*, *21*, 611–619.

Déry, S. J., and R. D. Brown (2007), Recent Northern Hemisphere snow cover extent trends and implications for the snow-albedo feedback, *Geophys. Res. Lett.*, *34*, L22504, doi:10.1029/2007GL031474.

Fernandes, R., G. Pavlic, W. Chen, and R. Fraser (2001), Canada-wide 1-km water fraction, National Topographic Database, www.nrcan.gc.ca/ess/_portal_esst.cache/gc_ccrs_e, Nat. Resour. Can., Ottowa, Ont.

Flanner, M. G., C. S. Zender, P. G. Hess, N. M. Mahowald, T. H. Painter, V. Ramanathan, and P. J. Rasch (2009), Springtime warming and reduced snow cover from carbonaceous particles, *Atmos. Chem. Phys. Discuss.*, *9*, 2481–2497.

Fowler, C., J. Maslanik, T. Haran, T. Scambos, J. Key, and W. Emery (2000), *AVHRR Polar Pathfinder twice-daily 5 km EASE-grid composites*, Natl. Snow and Ice Data Cent., Boulder, Colo., (Available at http://nsidc.org/data/docs/daac/nsidc0066_avhrr_5km.gd.html).

Graversen, R. G., and M. Wang (2009), Polar amplification in a coupled climate model with locked albedo, *Clim. Dyn.*, *33*, 629–643, doi:10.1007/s00382-009-0535-6.

Groisman, P. Y., T. R. Karl, and R. W. Knight (1994), Changes of snow cover, temperature and radiative heat balance of the Northern Hemisphere, *J. Clim.*, *7*, 1633–1656, doi:10.1175/1520-0442(1994)007<1633:COSCTA>2.0.CO;2.

Hall, A. (2004), The role of surface albedo feedback in climate, *J. Clim.*, *17*, 1550–1568, doi:10.1175/1520-0442(2004)017<1550:TROSAF>2.0.CO;2.

Hall, A., and X. Qu (2006), Using the current seasonal cycle to constrain snow albedo feedback in future climate change, *Geophys. Res. Lett.*, *33*, L03502, doi:10.1029/2005GL025127.

Hall, A., X. Qu, and J. D. Neelin (2008), Improving predictions of summer climate change in the United States, *Geophys. Res. Lett.*, *35*, L01702, doi:10.1029/2007GL032012.

Intergovernmental Panel on Climate Change (2007), *Climate Change 2007: The Physical Science Basis. Contribution of Working Group I to the Fourth Assessment Report of the Intergovernmental Panel on Climate Change*, edited by S. Solomon et al., Cambridge Univ. Press, Cambridge, U. K.

Lian, M. S., and R. D. Cess (1977), Energy balance models: A reappraisal of ice-albedo feedback, *J. Atmos. Sci.*, *34*, 1058–1062, doi:10.1175/1520-0469(1977)034<1058:EBCMAR>2.0.CO;2.

Maslanik, J., C. Fowler, T. Scambos, J. Key, and W. Emery (1997), AVHRR-based polar pathfinder products for modeling applications, *Ann. Glaciol.*, *25*, 388–392.

Pielke, R. A., Sr., G. E. Liston, W. L. Chapman, and D. A. Robinson (2004), Actual and insolation-weighted Northern Hemisphere snow cover and sea-ice between 1973–2002, *Clim. Dyn.*, *22*, 591–595, doi:10.1007/s00382-004-0401-5.

Qu, X., and A. Hall (2006), Assessing snow albedo feedback in simulated climate change, *J. Clim.*, *19*, 2617–2630, doi:10.1175/JCLI3750.1.

Qu, X., and A. Hall (2007), What controls the strength of snow albedo feedback?, *J. Clim.*, *20*, 3971–3981, doi:10.1175/JCLI4186.1.

Robinson, D. A., and A. Frei (2000), Seasonal variability of Northern Hemisphere snow extent using visible satellite data, *Prof. Geogr.*, *52*, 307–315, doi:10.1111/0033-0124.00226.

Sellers, W. D. (1969), A Global climatic model based on the energy balance of the Earth-atmosphere system, *J. Appl. Meteorol.*, *8*, 392–400, doi:10.1175/1520-0450(1969)008<0392:AGCMBO>2.0.CO;2.

Simmons, A. J., and J. K. Gibson (2000), The ERA-40 project plan, *ERA-40 Proj. Rep. Ser. 1*, Eur. Cent. for Medium-Range Weather Forecasts, Reading, U. K.

Wang, X., and J. Key (2005), Arctic surface, cloud, and radiation properties based on the AVHRR Polar Pathfinder dataset. Part I: Spatial and temporal characteristics, *J. Clim.*, *18*, 2558–2574, doi:10.1175/JCLI3438.1.

Wexler, H. (1953), Radiation balance of the Earth as a factor in climatic change, in *Climatic Change*, edited by H. Shapley, pp. 73–105, Harvard Univ. Press, Cambridge, Mass.

Winton, M. (2006), Surface albedo feedback estimates for the AR4 climate models, *J. Clim.*, *19*, 359–365, doi:10.1175/JCLI3624.1.

Zhang, Y., W. B. Rossow, A. A. Lacis, V. Oinas, and M. I. Mishchenko (2004), Calculation of radiative fluxes from the surface to top of atmosphere based on ISCCP and other global datasets: Refinements of the radiative transfer model and the input data, *J. Geophys. Res.*, *109*, D19105, doi:10.1029/2003JD004457.

Zhao, H., and R. Fernandes (2009), Daily snow cover estimation from Advanced Very High Resolution Radiometer Polar Pathfinder data over Northern Hemisphere land surfaces during 1982–2004, *J. Geophys. Res.*, *114*, D05113, doi:10.1029/2008JD011272.

R. Fernandes and H. Zhao, Canada Centre for Remote Sensing, Earth Sciences Sector, Natural Resources Canada, 588 Booth St., Ottawa, ON K1A 0Y7, Canada. (richard.fernandes@nrcan.gc.ca)

A. Hall and X. Qu, Department of Atmospheric and Oceanic Sciences, University of California, Box 951565, Los Angeles, CA 90095, USA.

J. Key, NESDIS, NOAA, 1225 West Dayton St., Madison, WI 53706, USA.

X. Wang, Cooperative Institute for Meteorological Satellite Studies, University of Wisconsin-Madison, 1225 West Dayton St., Madison, WI 53706, USA.